Interannual Variations of South Atlantic Basin–Scale Circulation, Agulhas Eddy Propagation and the Regional Wind Field

Donna L. Witter and Arnold L. Gordon
Lamont–Doherty Earth Observatory of Columbia University
email: **dwitter@ldeo.columbia.edu**

Abstract

Variability of South Atlantic oceanic and atmospheric circulation is investigated from TOPEX/POSEIDON sea level observations and from NCEP reanalysis winds. Interannual variations of the large–scale and regional ocean circulation are identified from empirical orthogonal functions (EOFs) of gridded sea level fields and from propagation of Agulhas eddies observed in the alongtrack altimeter data. The first EOF mode of the basin–scale ocean circulation (54 percent of nonseasonal variance) corresponds to zonal shifts in the dome of sea level associated with the South Atlantic subtropical gyre. This mode indicates that there was a transition from a broad, flat gyre with weak western boundary flow and relatively strong flow on the eastern side of the basin in 1993 and 1994, to a more zonally compact gyre with stronger western boundary flow and weaker flow in the eastern third of the basin in 1996. Variations in the strength of the geostrophic circulation associated with this mode may play a role in the dispersal of Agulhas eddies across the South Atlantic. Eddies propagated primarily to the northwest in 1993 and 1994, when circulation in the northeastern part of the gyre was strong. Eddy propagation was more directly to the west in 1996, when circulation in the northeastern part of the gyre was weak. Singular value decomposition of the gridded sea level fields and winds from the NCEP reanalysis suggests that the observed variations

of basin–scale ocean circulation may be related to changes in the regional wind stress curl, with weak wind stress curl observed in 1993 and 1994 when gyre–scale circulation was sluggish, and stronger wind stress curl in 1996 when the gyre–scale circulation was more intense in the western two thirds of the basin. The correspondence between variations of the basin–scale circulation, Agulhas eddy propagation, and regional wind forcing suggest that the input of salt and vorticity to the South Atlantic subtropical gyre via Agulhas eddies may be partially controlled by interannual variations of the wind–forced, large–scale circulation. A modeling effort, aimed at elucidating the observed relationships between the basin–scale flow, eddy propagation, and regional wind field will be described.

Data Processing

General: A processed version of TOPEX/POSEIDON observations from cycles 9–171 (December 1992–May 1997) were obtained from V. Zlotnicki and A. Hyashi of the Jet Propulsion Laboratory. These alongtrack residuals were computed from the Geophysical Data Records after applying the Joint Gravity Model 3 orbits and Rapp mean sea surface, and applying corrections for ionospheric range delay, wet and dry tropospheric range delays, and inverse barometer effect. The TOPEX oscillator drift correction, pole tide correction, Gaspar 4.0 sea state bias correction, and a 147–mm TOPEX bias correction were also applied. The resulting values were interpolated to an alongtrack grid with uniform 6.2 km spacing. Additional processing removed the residual mean sea surface, ocean tides (UT 3.0 tide model), tidal aliases, and observations in regions shallower than 1000 m. A 1–d loess filter removed variability on time–scales shorter than 30 days.

Alongtrack data: A semi–automated version of the technique described by Byrne et al. (1995) was used to track eddy propagation in the alongtrack observations. This procedure identifies and tracks eddies based on their characteristic spatial and temporal patterns.

Gridded sea level fields: To isolate large–scale variability, sea level fields were gridded by applying a spatial loess smoother (see Greenslade et al., 1997) to the alongtrack data. This smoother significantly reduced variability on scales smaller than about 800 km, including variability associated with Agulhas eddies. The analysis of Agulhas eddies from the alongtrack data (Figs. 4–5) are therefore quasi–independent of the analyses of basin–scale circulation (Figs. 2, 6, 7) from the gridded sea level fields.

A note about the steric contribution to sea level: As discussed by Stammer (1997), estimates of the steric contribution to sea level in the South Atlantic subtropical gyre are poor, as they are based on sparse in situ data. In this work, an annual harmonic was removed from the along–track sea level at each location to reduce the steric contribution to total sea level variability. A zonal average was then removed from the gridded fields at each time to reduce thermal residuals that cannot be modeled as a simple annual cycle. This procedure removes any dynamical variations of sea level on annual timescales, as well as the zonally uniform component of steric variability on interannual and other timescales. Because annual variability represents a significant fraction of the total sea level variability of the South Atlantic (Chelton et al., 1990), the filtered data set is well suited for studying the less energetic, interannual variations of interest to this study. The contribution of residual steric effects to interannual variations of sea level (particularly EOF 1 below) was estimated and is discussed in detail in Witter and Gordon (1999).

South Atlantic Time–Mean Circulation
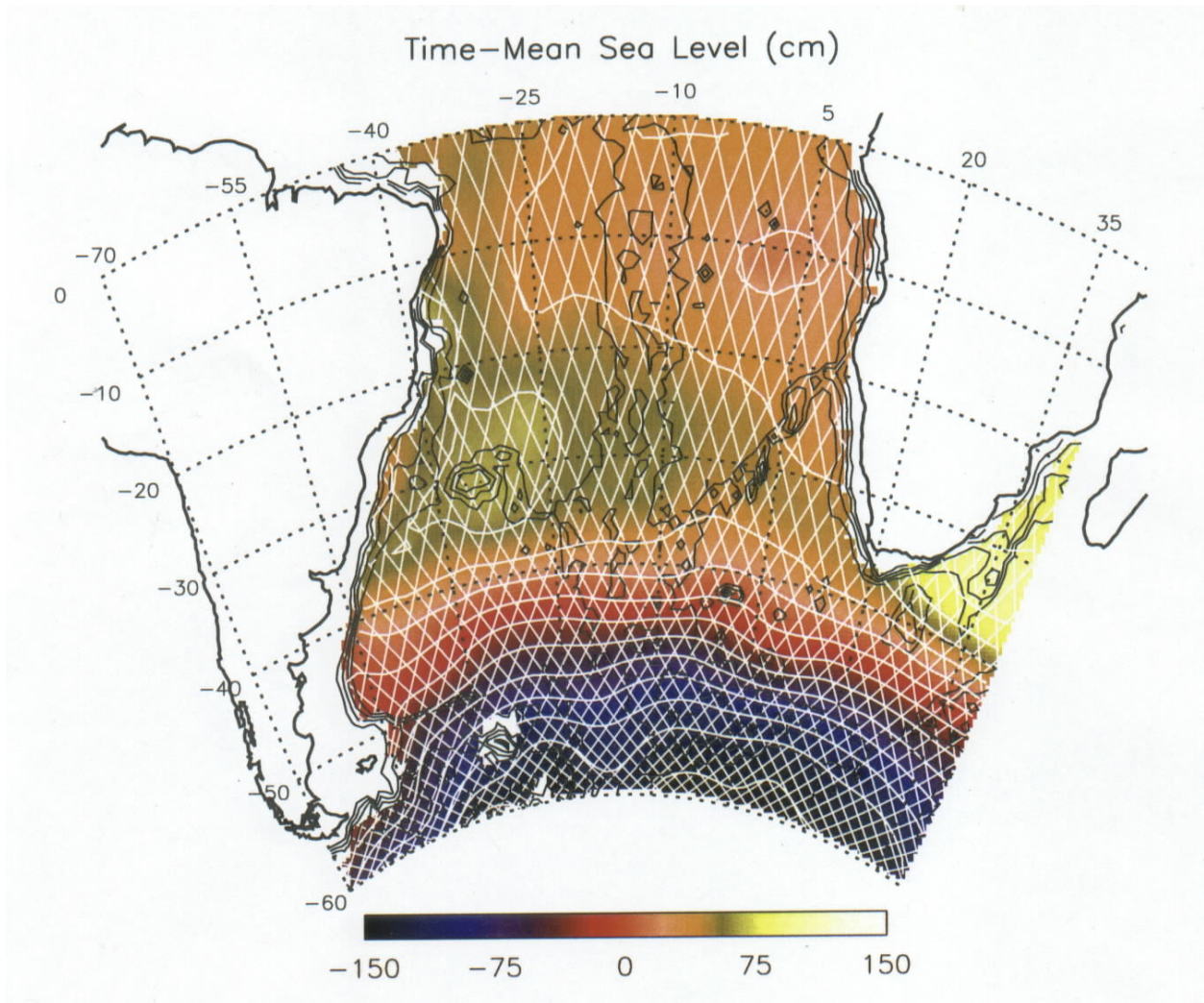
Fig. 1: Time–mean dynamic height computed from T/P observations relative to the JGM–3 geoid (ci=10 cm). Bathymetry contours are plotted as thin black lines (ci=500 m). The T/P ground tracks are plotted as thin white lines. The details of circulation in the boundary regions (e.g., the Brazil–Malvinas Confluence and the Agulhas Retroflection) are not resolved by the smoother used to grid the time–mean field or by the geoid.

Basin–Scale Sea Level Variability:
EOF Modes

The spatial pattern of EOF 1 (Fig. 2, top left) corresponds to changes of the large–scale circulation of the subtropical gyre. Anomalously high sea level occurs over the eastern third of the gyre at times when sea level is anomalously low near the western boundary. Temporal variations (Fig. 2, bottom left) of geostrophic velocity associated with mode 1 indicate enhanced circulation in the eastern South Atlantic in 1993 and 1994, followed by a transition in mid–1995 through mid–1996 to a state of more sluggish flow. The location of maximum sea level anomalies in the eastern part of the domain (i.e., the reversed ''C''–shaped pattern) corresponds well with the time–mean location of the eastern limb of the gyre (Fig. 1). This mode therefore represents interannual variations in the zonal extent of the region of strong subtropical gyre circulation. The dome of sea level associated with the gyre is broad and flat in 1993 and 1994, when the gyre is displaced to the east of its time–mean position. The dome of sea level associated with the gyre is taller and shifted toward the western boundary in 1996. The smoothed signature of Brazil Current velocities associated with mode 1 are correspondingly larger in 1996.
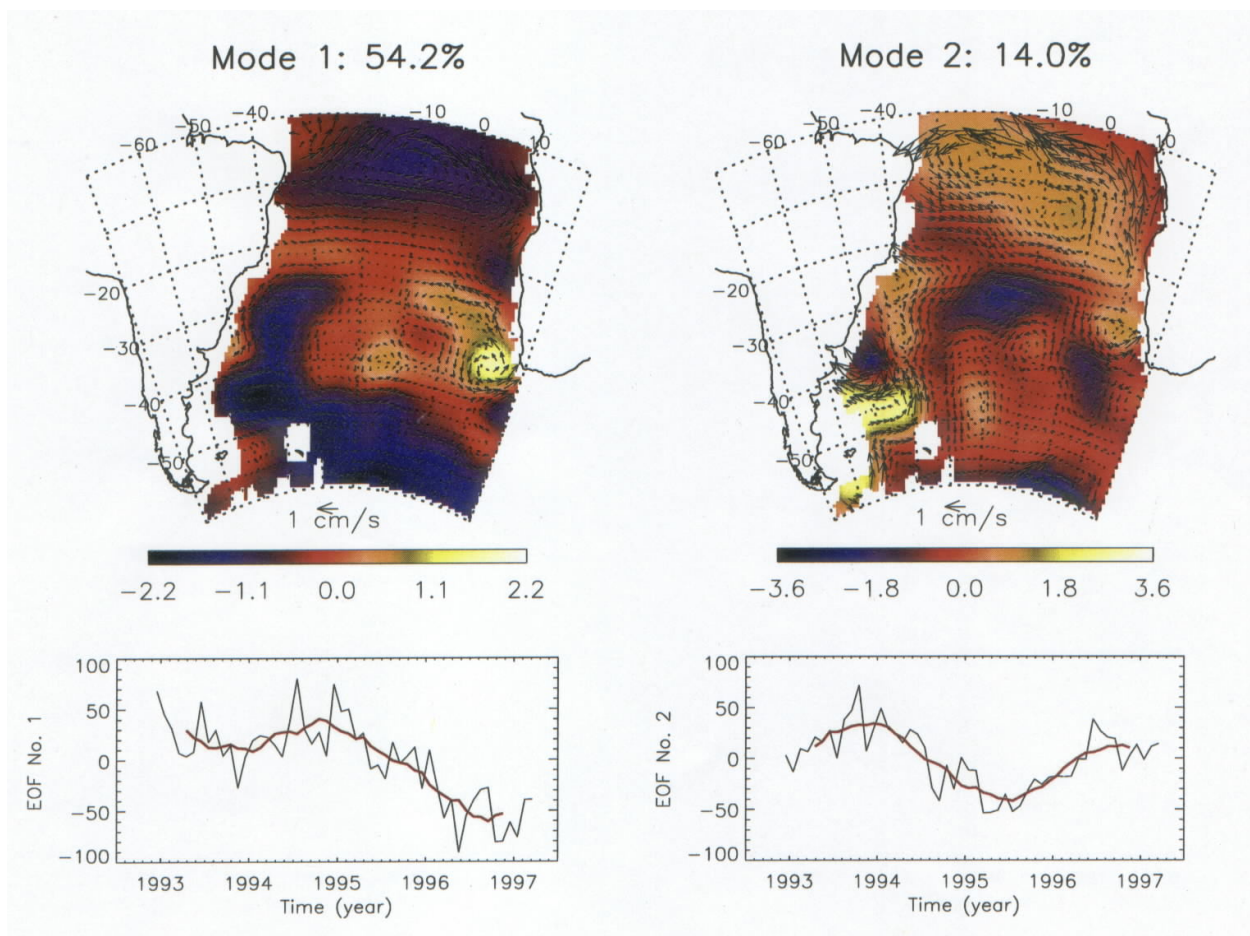
Fig. 2: (top) Spatial patterns of the first two basin–scale sea level modes (color images), the corresponding geostrophic velocity fields (vectors), and (bottom) amplitude time series (black lines). The color bar indicates the sea level (in cm) when the amplitude time series is equal to 30.0. The 9–month running average of the amplitude time series is plotted in red (bottom).

Eddy Propagation in the Cape Basin

A total of 21 large–amplitude, long–lived eddies were identified from the alongtrack data (Fig. 3). Excluding eddies that were first observed at cycle 9 or last observed at cycle 171, each eddy was tracked for an average of 1.7 years over which it translated by 23.6 degrees longitude and 5.0 degrees latitude and its amplitude decayed by 12.8 cm. On average, 4.8 eddies were observed crossing the Walvis Ridge per year.

Eddies crossed the Walvis Ridge at irregular intervals, as expected from the irregular shedding of eddies observed previously at the Retroflection (see Goni et al., 1997).
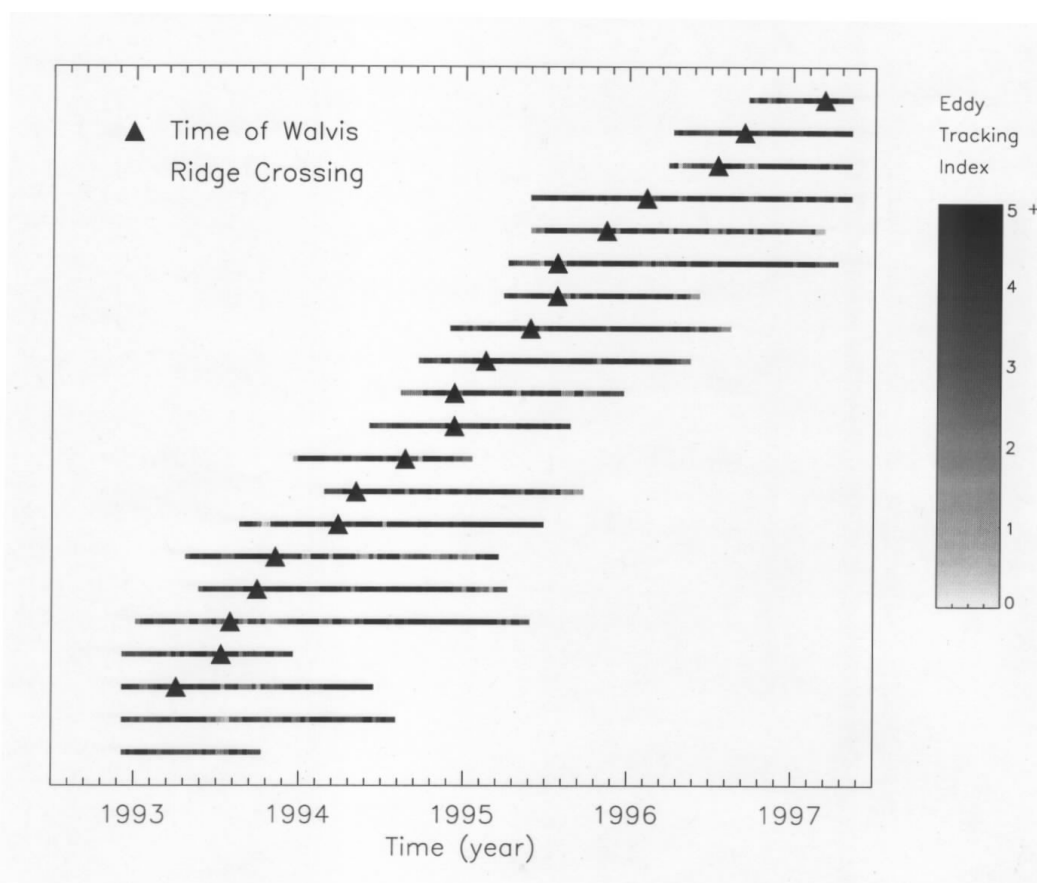
Fig. 3: Agulhas eddies extracted from T/P alongtrack data. Each eddy is depicted by a horizontal bar, where the interval along the x−axis corresponds to the time period for which the eddy was tracked. At each time, the shading on the bar corresponds to the ratio between the eddy amplitude and the amplitude of sea level variability in a region within 3 deg latitude and longitude of the eddy (the "eddy tracking index"). Darker shades correspond to better eddy−tracking conditions. Triangles show the time at which each eddy crossed the Walvis Ridge. The first two eddies crossed the Walvis Ridge before the beginning of the data set.

Year−to−Year Variations of Eddy Propagation

The T/P observations demonstrate that the location of the "Agulhas Eddy Corridor" (the region over which Agulhas eddies are detected as they fan out across the South Atlantic Subtropical Gyre) varies on interannual time scales (Fig. 4).   In 1993 and 1994, eddies propagated from the Cape Basin into the interior of the gyre over a broad range of latitudes. In 1996, only one decaying feature was observed at the interior of the gyre south of 30S and fewer eddies were observed north of 25S, suggesting that the eddy narrowed between 1994 and 1996. A shift in the direction of propagation occurs in conjunction with this narrowing. In 1993 and 1994 eddies located west of 0 degrees have a strong northward component to their motion. This northward component is significantly reduced, and eddies propagated more directly to the west.
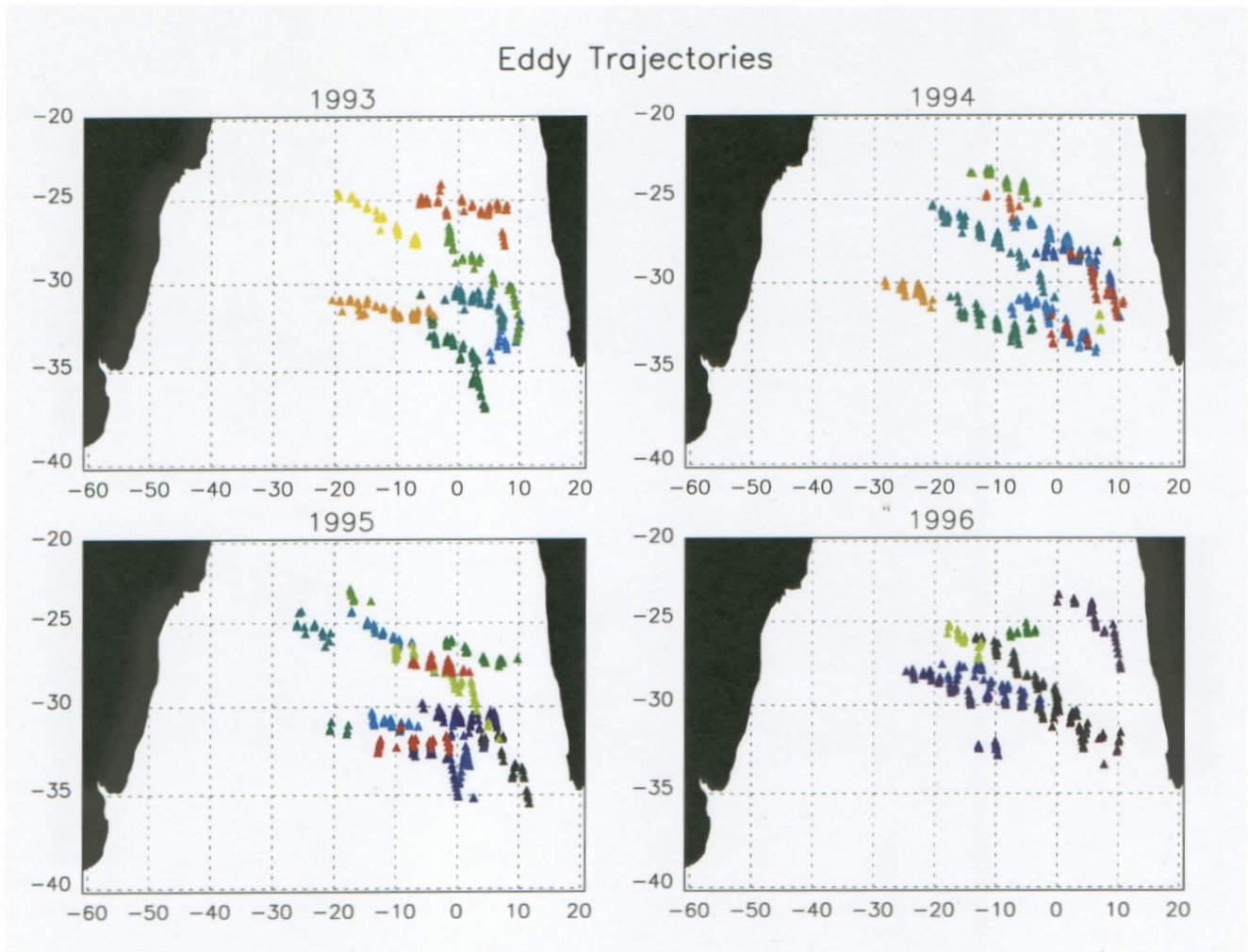
Fig. 4: Agulhas eddy trajectories computed from T/P observations for 1993, 1994, 1995, and 1996. The location of each eddy is marked with a symbol; each eddy is plotted as a different shade. Note the change from a broad Agulhas eddy corridor during 1993 and 1994 to a narrower corridor in 1996. In 1996, the eddy near 10E, 25S was detected late in the year and may suggest a return to a broader eddy corridor in 1997.

Surface Flow from Sea Level Mode 1:
Does Large–Scale Advection Influence Eddy Propagation?

Interannual variations of the location of the eddy corridor (Fig. 4) may be a response to variations of the large–scale ocean circulation. Zonal and meridional geostrophic velocity anomalies reconstructed from EOF 1 (Fig. 5) suggest that large–scale advection in the northeast (NE) quadrant of the gyre was stronger than usual in 1993 and 1994. Advection in the NE quadrant of the gyre was weaker than usual in 1996, when eddies propagated more directly to the west.
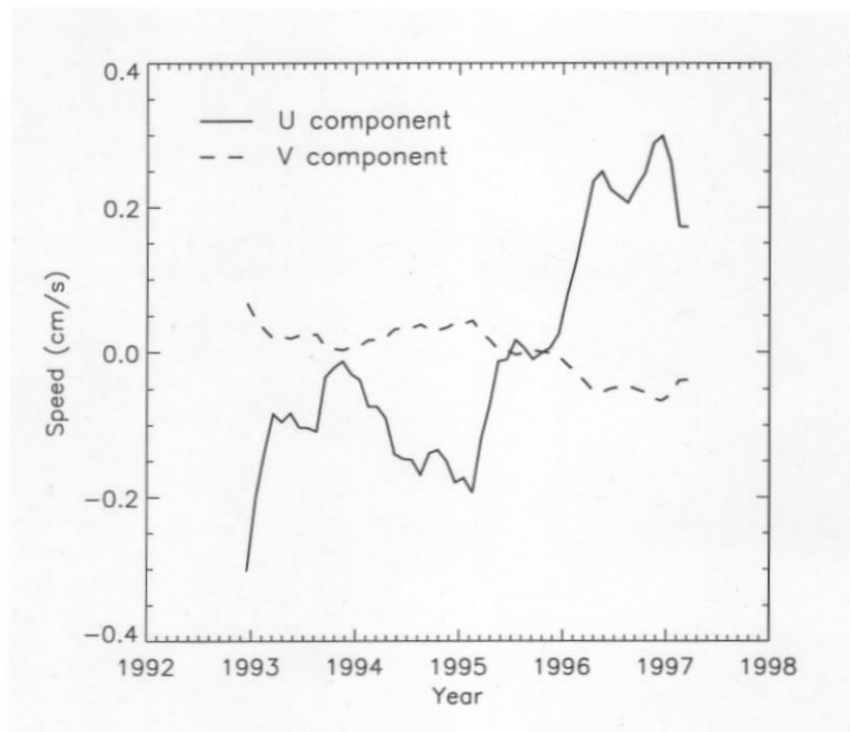
Fig. 5: Anomalies of zonal (solid line) and meridional (dashed line) geostrophic velocity components reconstructed from the first EOF of basin–scale sea level variability (see Fig. 2). Velocity components are averaged in a region northwest of the Cape Basin (10W–10E, 20S–30S). The time–mean flow in this region is to the northwest (see Fig. 1). Negative zonal velocity anomalies reinforce the zonal component of time–mean flow; positive zonal velocity anomalies oppose the zonal component of the time–mean flow.

Sea Level and Zonal Wind Covariability

Analysis of covariability between sea level and the near–surface wind based on singular value decomposition (SVD, see Fig. 6) suggests a mechanism for the variations of gyre–scale circulation associated with EOF 1. The spatial correlation between the pattern of sea level from SVD mode 1 (Fig. 6, top left) and the pattern of sea level EOF 1 (Fig. 2, top right) is remarkably strong (0.94). This high correlation suggests that the zonal wind pattern shown in Fig. 6 (top left) is associated with the gyre–scale sea level variations and, possibly, with the year–to–year variations of Agulhas eddy trajectories shown in Fig. 4.
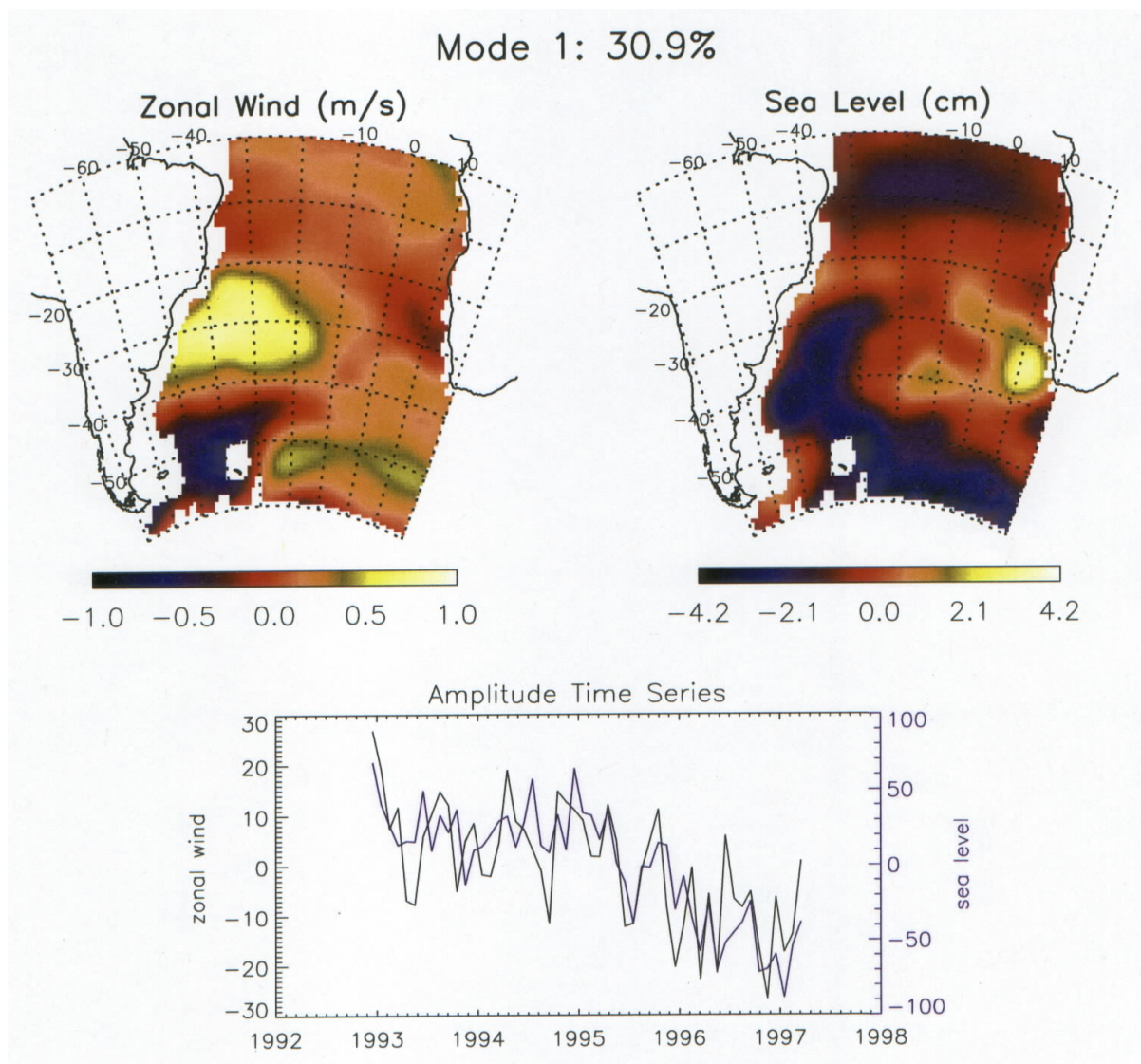
Fig 6: Leading mode of basin–scale zonal wind and sea level covariability computed from singular value decomposition of the T/P gridded sea level and contemporaneous, monthly, near–surface zonal wind fields from the NCEP reanalysis (Kalnay et al., 1996). The top panels show the spatial patterns of zonal wind (left) and sea level (right). Corresponding time series are shown in the bottom panel. Zonal wind and sea level fields in the top panels are plotted for amplitudes equal to 10 and 30, respectively. To focus on interannual variations, the zonal wind fields were smoothed to eliminate small–scale variability and an annual and semiannual harmonic were removed at each location.

A Link to the Large–Scale Wind Stress Curl?

To explore the possible link between variations of gyre–scale circulation and variations of the wind, a quantity somewhat analogous to the contribution of the SVD mode 1 zonal wind pattern to the zonal component of wind stress curl is plotted in Fig. 7. (Note that calculating the contribution of zonal wind mode 1 to the true wind stress curl requires an estimate of interannual variations in near–surface atmospheric stability. In the South Atlantic, these observations are considerably less reliable than observations of the wind components alone.) The resulting field (Fig. 7) suggests that interannual variations of gyre–scale circulation are associated with variations of the large–scale wind stress curl. During 1993 and 1994, the zonal wind variability of SVD mode 1 (Fig. 6, top left) opposes the time–mean wind pattern, reducing the large–scale positive wind stress curl. In 1996, the zonal wind variability of SVD mode 1 reinforces the time mean wind pattern, increasing the large–scale positive wind stress curl.

In a previous study of the wind–forced circulation of the South Atlantic basin (Matano et al., 1993), the intensity of circulation about the gyre and the zonal extent of the gyre–scale circulation was sensitive to variations of wind stress curl on seasonal time scales. Results from this analysis of T/P data suggest that a similar mechanism may operate on interannual time scales, with the additional potential impact on Agulhas eddy propagation, a process which has no seasonal analog.

Meridional Gradient of Mode 1 Zonal Wind

$-du/dy \ 10^{-6} \ 1/s$
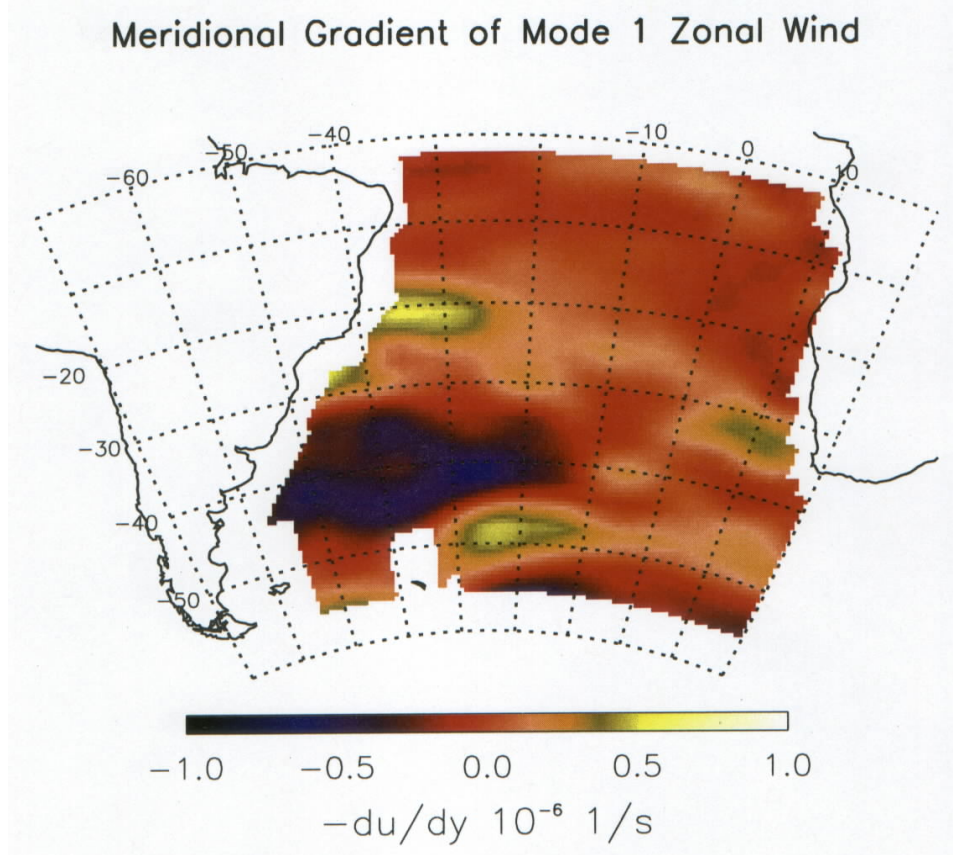
Fig. 7: Negative of the meridional gradient of the zonal wind pattern shown in Fig. 6 This field suggests that interannual variations of gyre–scale circulation are associated with variations in the large–scale wind stress curl. During 1993 and 1994, the zonal wind variability of SVD mode 1 (Fig. 6, top left) opposes the time–mean wind pattern and the large–scale positive wind stress curl is reduced. In 1996, the zonal wind variability of SVD mode 1 reinforces the time mean wind pattern and the large–scale positive wind stress curl is increased.

A Modeling Study

The possible link between the large–scale circulation of the South Atlantic gyre, the regional wind field, and Agulhas eddy propagation has motivated a modeling study to investigate these links in more detail. This study uses the Lamont Ocean–Atmosphere mixed layer Model (LOAM). The Lamont Ocean–Atmosphere Mixed Layer Model, an extension of the primitive equation model of Gent and Cane (1989), solves the primitive equations on an A–grid and is forced by wind stress. Fresh water fluxes are obtained by restoring the sea surface salinity to observations. This model is configured for the South Atlantic domain (with an extension into the western Indian Ocean); a stretched grid provides enhanced horizontal resolution in the Agulhas Retroflection and Cape Basin Regions. The primary goals of the model experiments are to investigate:

   (a) interannual variability of Agulhas eddy propagation,

   (b) the link between this variability and variability of the gyre–scale circulation,

   (c) the effect of low–frequency wind variations on Agulhas eddy propagation and gyre–scale circulation, and

   (d) links between observed variability of both the gyre–scale circulation and Agulhas eddies and the thermohaline circulation of the South Atlantic basin.

Model Configuration and Processes
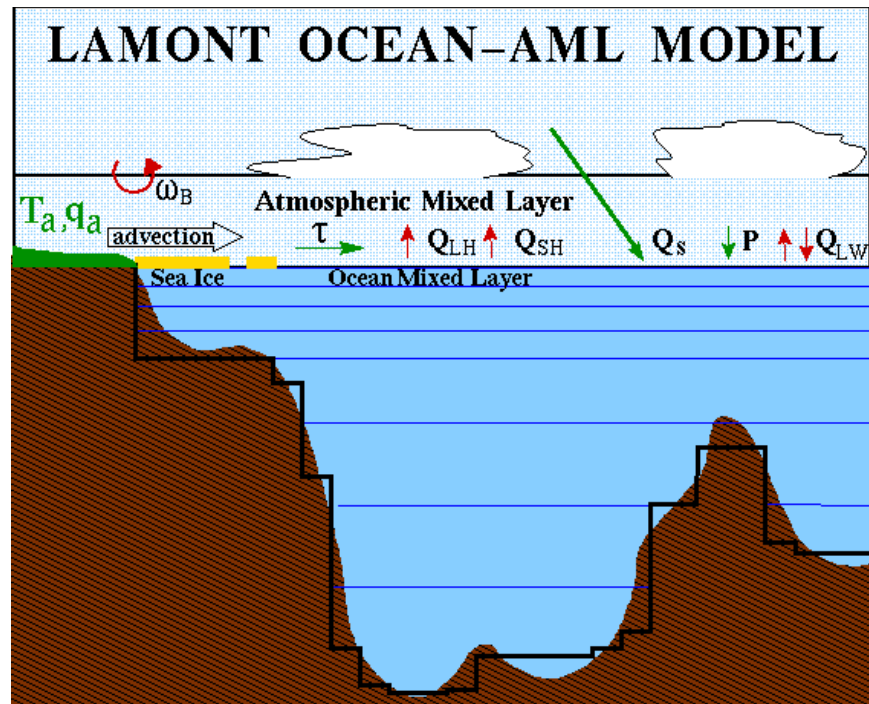
Model Domain and Bathymetry
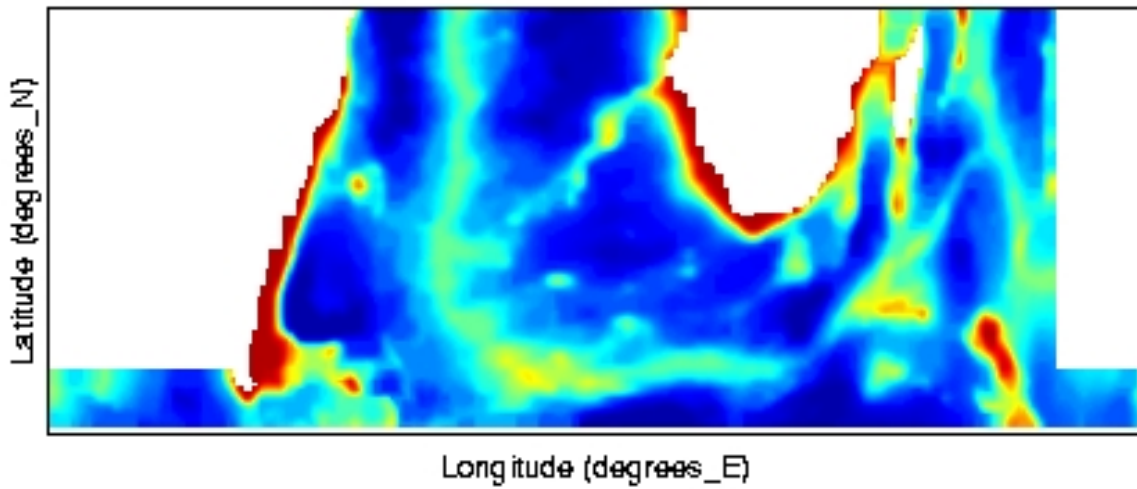
References

Byrne, D., A.L. Gordon, and W. Haxby, Agulhas eddies: A synoptic view using Geosat ERM data, J. Phys. Oceanogr., 25, 902––917, 1995.

Chelton, D.B., M.G. Schlax, D.L. Witter, and J.G. Richman, Geosat altimeter observations of the surface circulation of the Southern Ocean, J. Geophys. Res., 95, 17,877–17,903, 1990.

Gent, P.R., and M.A. Cane, 1989: A reduced gravity, primitive equation model of the upper equatorial ocean. J. Comput. Phys., 81, 444––480.

Goni, G.J., S.L. Garzoli, A.J. Roubicek, D.B. Olson, and O.B. Brown, Agulhas ring dynamics from TOPEX/POSEIDON satellite altimeter data, J. Mar. Res., 55, 861–883, 1997.

Greenslade, D.J.M., D.B. Chelton, and M.G. Schlax, The midlatitude resolution capability of sea level fields constructed from single and multiple satellite altimeter datasets, J. Atmos. Oceanic Technol., 14, 849–870, 1997.

Kalnay, E. et al., The NCEP/NCAR 40–year reanalysis project, Bull. Am. Meteorol. Soc., 77, 437–471, 1996.

Matano, R.P., M.G. Schlax, D.B. Chelton, Seasonal variability in the Southwestern Atlantic, J. Geophys. Res., 98, 18,027 18,036, 1993.

Stammer, D., Steric and wind–induced changes in TOPEX/POSEIDON large–scale sea surface topography observation, J. Geophys. Res., 102, 20,987–21,009, 1997.

Witter, D.L., and A.L. Gordon, 1999: Interannual variability of South Atlantic circulation from four years of TOPEX/POSEIDON satellite altimeter observations. J. Geophys. Res., 104, 20927–20948.